Supporting Information

Nuclear receptor RORα regulates pathologic retinal angiogenesis by modulating SOCS3-dependent inflammation

Ye Sun[a], Chi-Hsiu Liu[a], John Paul SanGiovanni[b], Lucy P. Evans[a], Katherine T. Tian[a], Bing Zhang[c], Andreas Stahl[d], William T. Pu[c], Theodore M. Kamenecka[e], Laura A. Solt[e], and Jing Chen[a,1]

[a]Department of Ophthalmology, Harvard Medical School, Boston Children's Hospital, Boston, MA 02115; [b]Section on Nutritional Neuroscience, National Institute on Alcohol Abuse and Alcoholism, Bethesda, MD 20892; [c]Department of Cardiology, Boston Children's Hospital, Boston, MA 02115; [d]Eye Center, University of Freiburg, 79106 Freiburg, Germany; and [e]Department of Molecular Therapeutics, The Scripps Research Institute, Jupiter, FL 33458.

[1]To whom correspondence should be addressed. Email: jing.chen@childrens.harvard.edu.

SI Materials and Methods

Animals

The retinas from *Cx3cr1-GFP* mice (Jackson Lab, stock # 005582) in which the insertion of sequence encoding green fluorescent protein (GFP) disrupted and replaced an endogenous *Cx3cr1* locus, were kindly provided by Dr. Martin Friedlander's group.

Analysis of Oxygen-induced Retinopathy (OIR)

OIR was carried out in neonatal RORα deficient staggerer mice (*Sg/Sg*) or wild type (WT) mice as described previously (1-4), with mouse pups exposed to 75% oxygen at postnatal day (P) 7 - P12 followed by room air (**Figure 1A**). At P17, mice were anesthetized, and retinas dissected followed by fluoresceinated isolectin IB_4 (*Griffonia simplicifolia*) (Invitrogen) staining to visualize vessels on whole-mount retinas. Areas of retinal vasoobliteration (VO) and pathologic neovascularization (NV) were quantified as a percentage of total retinal areas using Adobe Photoshop and Image J (National Institutes of Health, http://imagej.nih.gov/ij/). SR1001 (25mg/kg body weight) and SR1078 (10 mg/kg body weight) or vehicle controls were injected intraperitoneally in C57BL/6J OIR littermate mice from P12-P17 twice per day. Both SR1001 and SR1078 were synthesized at the Scripps Research Institute (5, 6). Mice treated with SR1001 and SR1078 had comparable body weight as controls. *Sg/Sg* mice and WT mice were maintained within normal range of body weight for OIR (5-7.5 grams at P17) (7) through adjusting litter size. Mice with very low body weight (less than 5 grams at P17) were excluded from the study, which we have found impacts OIR outcomes with delayed neovascularization and exaggerated vasoobliteration (7).

Analysis of *Vldlr*$^{-/-}$ Mice

For retinal mRNA expression, *Vldlr*$^{-/-}$ and WT retinas were collected from P7 and P17 mice, followed by RNA isolation and RT-qPCR according to the methods described in sections below. For SR1001 treatment, *Vldlr*$^{-/-}$ pups were intraperitoneally injected with SR1001 (25mg/kg body weight) or vehicle treatment in littermate controls from P5 to P15 twice per day. At P16, mice were anesthetized, retinas were dissected, collected either for RNA analysis or fixed in 4% paraformaldehyde followed by staining with fluoresceinated isolectin IB_4 to visualize subretinal neovascularization in flat-mounted retinas. Retinas were mounted onto Superfrost/Plus microscope slides (Fisher Scientific) with the photoreceptor side up. Flat mounts were imaged at 10X magnification with AxioObserver.Z1 microscope (Zeiss) with a monochrome digital camera (AxioCam MRm; Zeiss) focusing on the lesions. Individual images were merged to create one entire retinal image using the automated merge function (mosaiX; Zeiss) in the software (AxioVision 4.6.3.0; Zeiss). 3D reconstructed images were taken with confocal microscopy (Leica TCS SP2 AOBS) and z-stacks were 3D reconstructed using Volocity software (Perk Elmer). For quantification of subretinal neovascularization lesion counts and areas, Image J was used with designed plugins adapted from the method used to measure retinal neovascularization (SWIFT_NV) in the OIR model (8). This plugin with a set of macros uses a user-designated intensity threshold to mark lesion structures that clearly stand out from background fluorescence of normal vessels, and can automatically remove small artifacts like vessel branching points or tiny debris by selecting objects with a minimum size of 100 pixels. Other artifacts such as occasional cellular debris or retinal periphery with hyperfluorescence can be manually excluded from quantification when needed. Lesion counts and areas were quantified in a blinded fashion with researchers masked to the identity of samples.

Aortic Ring Sprouting Assay

Aortae from 2-month-old WT and RORα deficient mice *Sg/Sg* were dissected and cut into 1-mm-long pieces.

Aortic rings were placed in growth factor–reduced Matrigel (BD Biosciences) and cultured for 5 days in EBM-2 medium (Lonza) (9, 10). Images of individual aortic explants were taken and the microvascular sprouting areas were quantified by measuring the area covered by outgrowth of the vascular sprouts with Image J.

Macrophage RAW 264.7 Cell Culture

The murine macrophage cell line, RAW 264.7, was obtained from ATCC (catalog # TIB-71) and maintained in DMEM containing 10% heat inactivated FBS (Invitrogen) and antibiotics. For RORα inhibition, cells were transfected with siRNA targeting RORα (*siRora*) or control siRNA (*siControl*) (Ambion) using siLentFect (Bio-RAD) for 48 hours before collected for RNA extraction. For *Socs3* inhibition, lentivirus expressing *Socs3* shRNA (lenti-*shSocs3*) were incubated with cells overnight along with 8% polybrene and on day 2 the medium were changed to complete culture medium. On day 4 the cells were collected for RNA extraction. For SR1001 or SR1078 treatment, cells were treated with SR1001 (5 or 10 μM), or SR1078 (10 or 20 μM) in DMSO or control (DMSO) overnight and collected for RNA extraction.

Coculture of Aortic Rings and Macrophage RAW 264.7 Cells

Culture of aortic ring and macrophage was described separately in supplemental materials. Co-culture were performed with a transwell system, with aortic rings cultured at the bottom of wells before addition of pretreated RAW 264.7 cells to the top of transwells. RAW 264.7 cells were pre-treated with lenti-*shControl* or lenti-*shSocs3* for overnight, followed by transfection with *siControl* or *siRora*. At day 5, the pretreated RAW 264.7 cells were added into transwell on the top of the wells with aortic rings growing at the bottom (10,000 RAW 264.7 cells per ring). Aortic ring sprouting were imaged at day 8 and quantified.

Intravitreal Injection of Lentivirus or Liposome

Intravitreal injections were performed by inserting an Exmire microsyringe (MS-NE05, ITO Corp.) with 35-gauge needle into the vitreous 1 mm posterior to the corneal limbus (11). Intravitreal injection of lentivirus expressing *Socs3* shRNA (Lenti-*shSocs3*) was performed at P5 in *Sg/Sg* and WT mice with 0.5 μl of Lenti-*shControl* or Lenti-*shSocs3* injected in contralateral eyes before mice were subjected to OIR. Intravitreal injection of liposome was performed with 0.5 μl of clodronate-liposome (containing 5mg/ml of clodronate) or control PBS-liposome from Clodronate Macrophage Depletion Kit (Encapsula NanoScience LLC), injected in contralateral eyes of *Sg/Sg* and WT mice at P12 after mice were subjected to OIR.

RNA Isolation and Quantitative RT-PCR

Total RNA was extracted from mouse retinas using RNeasy kit (Qiagen) and reverse-transcribed with M-MLV reverse transcriptase (Invitrogen) to generate cDNA. Quantitative PCR was performed using a 7300 system (Applied Biosystems) with KAPA SYBR FAST qPCR Kits (Kapa Biosystems). Primer sequences were list in supplementary Table S1.

Immunohistochemistry

Immunostaining in retinas was performed as described previously (11, 12). Briefly, eyes were isolated from P17 C57BL/6J or *Cx3cr1-GFP* mice with OIR and fixed in 4% paraformaldehyde for 1 hour. Dissected retinas were placed in cold methanol for 20 minutes, blocked, and permeabilized in phosphate buffered saline (PBS) containing 5% goat serum and 0.3% Triton X-100 for 1 hour. The retinas were stained with isolectin IB_4, flat-mounted on slides and imaged with Olympus Fluoview 1000 confocal microscope. The following antibodies were used: RORα antibody (Abcam, catalog # ab60134), CD11b (BioLegend, catalog # 101201) and F4/80 (Bio-Rad AbD Serotec, MCA497A488).

Chromatin Immunoprecipitation (ChIP) Assay

ChIP assay was performed using a ChIP assay kit (Upstate, Millipore) according to the manufacturer's protocol, with minor modifications. The ChIP assay was repeated three times. Briefly, for each ChIP assay, 30 retinas from P17 C57BL/6J mice with OIR were dissected and pooled in 10 ml ice cold PBS with protease inhibitor cocktail (Roche). Chilled retinas were dissociated and crosslinked with 1% formaldehyde for 20 minutes at room temperature with agitation. Retinas were incubated for an additional 5 minutes in 125 mM glycine and rinsed twice with ice cold PBS. Retinas were lysed and sonicated on ice using a Misonix Sonicator 3000. Retina lysates were pre-cleaned using a salmon sperm DNA/protein A agarose-50% slurry and immunoprecipitation was performed overnight with 4 μg of RORα antibody at 4 degree with agitation. DNA fragments bound to RORα antibody were eluted from agarose beads with SDS elution buffer (1% SDS, 50 mM Tris-HCl and 10 mM EDTA buffer) and incubated with 10 mg RNase A at 37 degree for 1 hour, proteins digested by incubation with proteinase K (20 mg/ml), at 55 degree for 1 hour. Precipitated DNA fragments were purified using QIAquick PCR purification kit. Input (control) samples were isolated similarly and incubated with pre-clean solution instead of RORα antibody or with rabbit IgG antibody (negative control). Real time PCR reactions were performed using diluted input, IgG control or experimental (RORα antibody precipitated) DNA fragments as template, and with primers designed flanking a putative RORE site in the potential target genes to amplify approximately 200 base pair products. Enrichment levels significantly higher than nonspecific negative control (*Hbb*), and comparable with or higher than positive control (*Opn1mw*) were considered positive enrichment threshold.

Western Blot

A standard immunoblotting protocol was used with minor modifications. Briefly, RIPA buffer (Cell Signaling) was used to lyse the retinal samples or cells. Protease inhibitor cocktail (Thermo Scientific, 78430) was added. Proteins were separated by electrophoresis using 4-12 %NuPAGE Novex Bis-Tris gels (Invitrogen). The primary antibodies used were: β-ACTIN (Sigma, A1978), SOCS3 (Santa Cruz, sc-9023) and RORα (Abcam, ab60134).

Luciferase Reporter Assay

DNA fragment containing putative RORE site in *Socs3* promoter regions (covering residues -2,310bp to -2,314bp region) was amplified from mouse genomic DNA with primers (supplementary Table S2), then cloned into luciferase report vector *pGL2*. Mutant construct of *Socs3* with deletion in RORE site (*Socs3*: -2,310bp to -2,314bp) was also constructed with luciferase reporter. HEK293T cells were transiently cotransfected with *pCDH1-Rorα-Flag*, wt or mutant *pGL2-Socs3* promoter reporter, or *Renilla* luciferase vector alone as control. For SR1001 treatment, SR1001 was dissolved in DMSO and the pre-transfected HEK293T cells were treated overnight. At 36 hours post-transfection, cells were lysed in passive lysis buffer (Promega, Dual-Luciferase assay system) and luciferase reporter activities measured using a Wallac 1420 Multilabel Counter (Perkin Elmer luminometer).

Statistics

Results were presented as mean ± SEM for animal studies and mean ± SD for non-animal studies. For animal studies, n is the number of retinas quantified. For all statistical analysis, F-tests (for two samples, or Levene's test for more than two samples) were performed first to assess whether the variance are homogenous. If the variances were homogenous, two-tailed t-tests (2 groups) or ANOVA (more than 2 groups) were performed assuming equal variances. For non-homogenous variances, two-tailed T-tests (or ANOVA) assuming unequal variances were performed. Differences were considered significant if $p \leq 0.05$. Data shown are representative of at least 3 independent experiments. * indicates $p<0.05$; ** indicates $p<0.01$; *** indicates $p<0.001$; n. s. indicates no significance.

References:

1. Smith LE*, et al.* (1994) Oxygen-induced retinopathy in the mouse. *Invest Ophthalmol Vis Sci* 35(1):101-111.
2. Stahl A*, et al.* (2010) The mouse retina as an angiogenesis model. *Invest Ophthalmol Vis Sci* 51(6):2813-2826.
3. Chen J*, et al.* (2011) Wnt signaling mediates pathological vascular growth in proliferative retinopathy. *Circulation* 124(17):1871-1881.
4. Michan S*, et al.* (2014) Sirtuin1 over-expression does not impact retinal vascular and neuronal degeneration in a mouse model of oxygen-induced retinopathy. *PLoS One* 9(1):e85031.
5. Wang Y, Solt LA, Kojetin DJ, & Burris TP (2012) Regulation of p53 stability and apoptosis by a ROR agonist. *PLoS One* 7(4):e34921.
6. Solt LA*, et al.* (2011) Suppression of TH17 differentiation and autoimmunity by a synthetic ROR ligand. *Nature* 472(7344):491-494.
7. Stahl A*, et al.* (2010) Postnatal weight gain modifies severity and functional outcome of oxygen-induced proliferative retinopathy. *Am J Pathol* 177(6):2715-2723.
8. Stahl A*, et al.* (2009) Computer-aided quantification of retinal neovascularization. *Angiogenesis* 12(3):297-301.
9. Sapieha P*, et al.* (2011) 5-Lipoxygenase Metabolite 4-HDHA Is a Mediator of the Antiangiogenic Effect of {omega}-3 Polyunsaturated Fatty Acids. *Sci Transl Med* 3(69):69ra12.
10. Li J*, et al.* (2014) Endothelial TWIST1 Promotes Pathological Ocular Angiogenesis. *Invest Ophthalmol Vis Sci* 55(12):8267-8277.
11. Chen J*, et al.* (2009) Suppression of retinal neovascularization by erythropoietin siRNA in a mouse model of proliferative retinopathy. *Invest Ophthalmol Vis Sci* 50(3):1329-1335.
12. Chen J*, et al.* (2013) Neuronal sirtuin1 mediates retinal vascular regeneration in oxygen-induced ischemic retinopathy. *Angiogenesis* 16(4):985-992.

Number of supplemental Tables: 2.

Number of supplemental Figures: 9.

Table S1 Primers for real time PCR

Gene	Forward (5'-3')	Reverse (5'-3')
Rora	TCCCACCTGGAAACCTGCCAGT	CCACGAGCGATCCGCTGACA
Socs3	AGCTGGTGGTGAACGCCGTG	GCGTGCTTCGGGGGTCACTC
Nos2	GTTCTCAGCCCAACAATACAAGA	GTGGACGGGTCGATGTCAC
Il6	TGGAGTCACAGAAGGAGTGGCTAAG	TCTGACCACAGTGAGGAATGTCCAC
Il1b	GCCCATCCTCTGTGACTCATG-21	GGAGCCTGTAGTGCAGCTGTCT-22
Cxcl10	CCAAGTGCTGCCGTCATTTTC	GGCTCGCAGGGATGATTTCAA
Tnf	CCAACATGCTGATTGATGACACC	GAGAATGCCAATTTTGATTGCCA
Il10	CTTACTGACTGGCATGAGGATCA	GCAGCTCTAGGAGCATGTGG
Fizz1	TCCAGCTAACTATCCCTCCACTGT	GGCCCATCTGTTCATAGTCTTGA
Ccl26	ATTTGGGTCTCCTTGTTCTC	GTAAAGAATATCACACCGTCACTG
Arg1	CTCCAAGCCAAAGTCCTTAGAG	AGGAGCTGTCATTAGGGACATC
Cx3cr1	GCAAGCTCACGACTGCCTT	TCCGGTTGTTCATGGAGTTGG

Table S2. Primers for Luciferase reporters

	Forward (5'-3')	Reverse (5'-3')
Socs3 WT	AAAAGCTAGCTAGTCAGTTTGCCCTCCTACTG	AAAACTCGAGGGTGATTGAGGTGAAAGGTTGTTTA
Socs3 MUT	GGTATCCAAGAGGGCATTGTCGAAAGCCCACTGAGA	TCTCAGTGGGCTTTCGACAATGCCCTCTTGGATACC

Figure S1

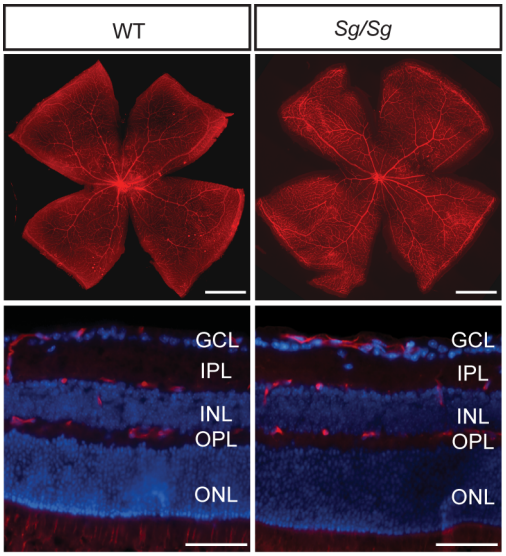

Figure S1. Normal retinal vasculature in adult WT and *Sg/Sg* mice. Upper panels: Retinal whole mounts stained with isolectin IB_4 from adult WT and *Sg/Sg* mice (2 month old). Lower panels: retinal cross sections of adult WT and *Sg/Sg* mice stained for endothelial cells with isolectin IB_4 (red) and cell nuclei with DAPI (blue). GCL: ganglion cell layer; IPL: inner plexiform layer; INL: inner nuclear layer; OPL: outer plexiform layer; ONL: outer nuclear layer. Scale bars: 1000 μm (upper panels) and 50 μm (lower panels).

Figure S2

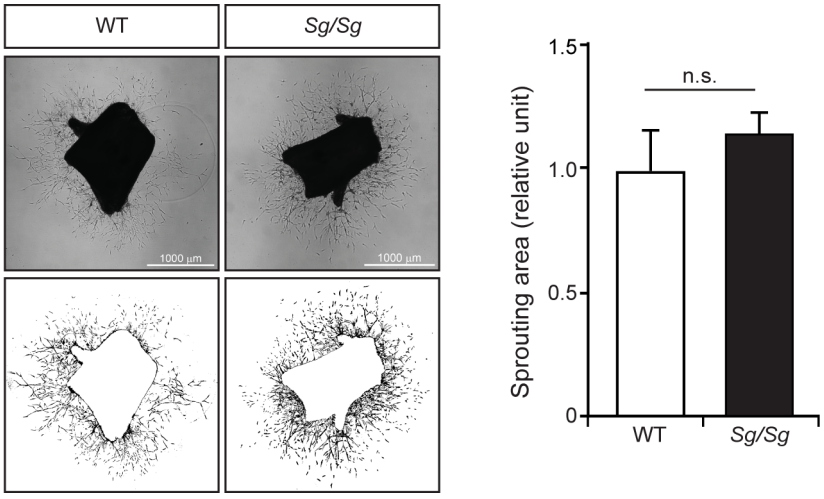

Figure S2. Vascular growth in aortic rings isolated from WT and *Sg/Sg* mice. Aortic ring assays were performed with fragments of aorta isolated from age-matched WT or *Sg/Sg* mice. Representative images were shown at the left. Right panels: areas of vascular sprouts were quantified from aortic rings imaged 5 days after explanting. No significant difference was observed in microvascular sprouting areas between WT and *Sg/Sg* mice. n.s.: no significance (n=6). Scale bars: 1000 μm.

Figure S3

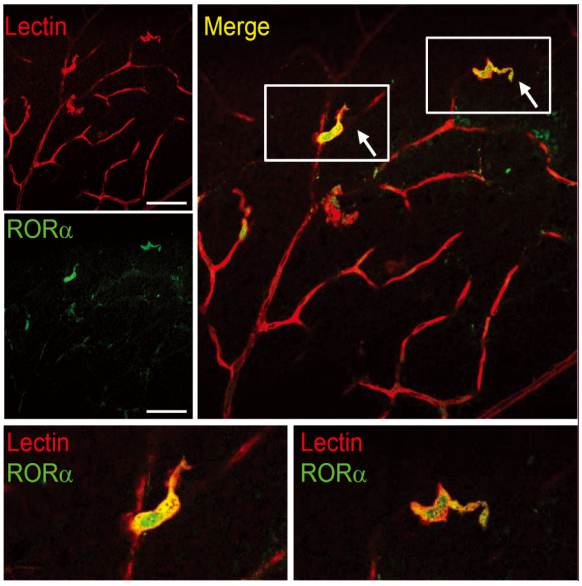

Figure S3. RORα staining was minimal in retinal blood vessels and present in vessel-associated cells resembling macrophages/microglia. P17 WT retinal whole mounts were stained with isolectin IB_4 (red) and RORα antibodies (green). RORα antibodies showed minimal visible staining in blood vessels, yet with strong staining in cells morphologically resembling macrophages/microglia (arrows in white box enlarged in lower panels). Scale bars: 50 μm.

Figure S4

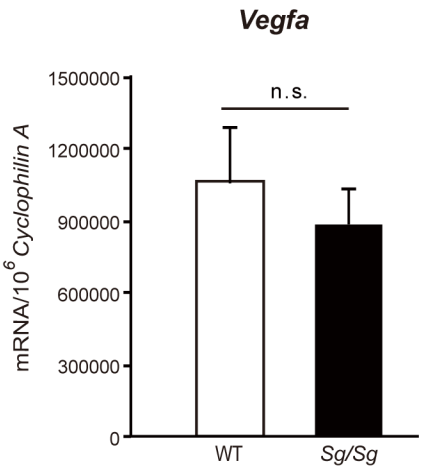

Figure S4. *Vegfa* expression was not significantly altered in *Sg/Sg* OIR retinas compared with WT. Expression of *Vegfa* was analyzed with qPCR in OIR WT and *Sg/Sg* retinas at P17 (n = 6 per group). Expression levels were normalized to house-keeping gene *Cyclophilin A*. n.s., no significance.

Figure S5

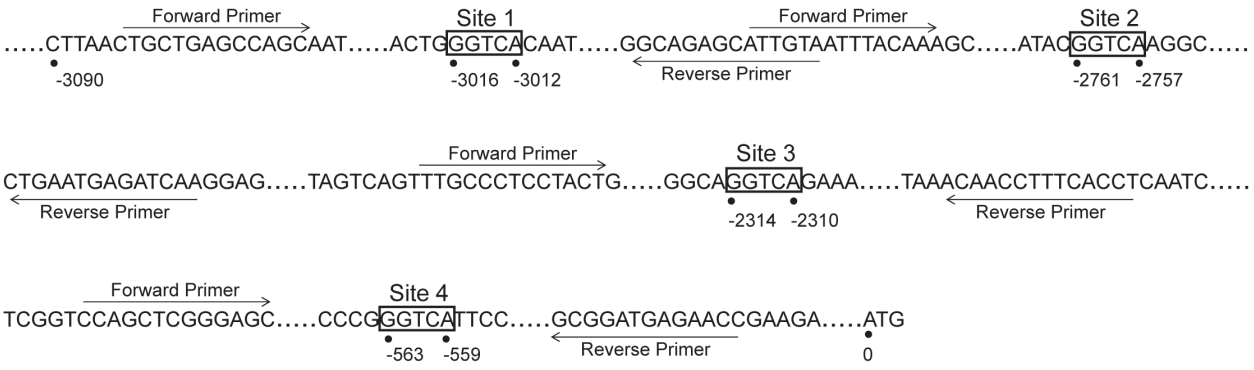

Figure S5. DNA sequence of *Socs3* promoter region with four potential RORE sites. Four putative RORE sites on *Socs3* promoter region and the primers used in ChIP assay were labeled. The numbers indicate the distance (in base pairs) for RORE sites on *Socs3* promoter from start codon ATG.

Figure S6

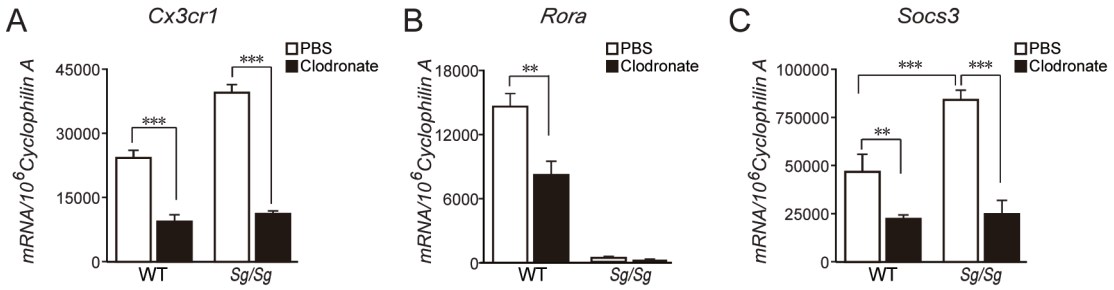

Figure S6. Macrophages depletion by clodronate liposome decreased *Rora* expression in the retina and abolished induction of *Socs3* expression in *Sg/Sg* OIR retinas. Expression of macrophage marker *Cx3cr1* (A), *Rora* (B) *and Socs3* (C) were analyzed with qPCR in WT control and *Sg/Sg* OIR retinas at P17 (n = 6 per group). Depletion of macrophages using clodronate liposome was confirmed by reduced levels of macrophage marker *Cx3cr1*. Expression levels were normalized to house-keeping gene *Cyclophilin A*. **, $p<0.01$; ***, $p<0.001$.

Figure S7

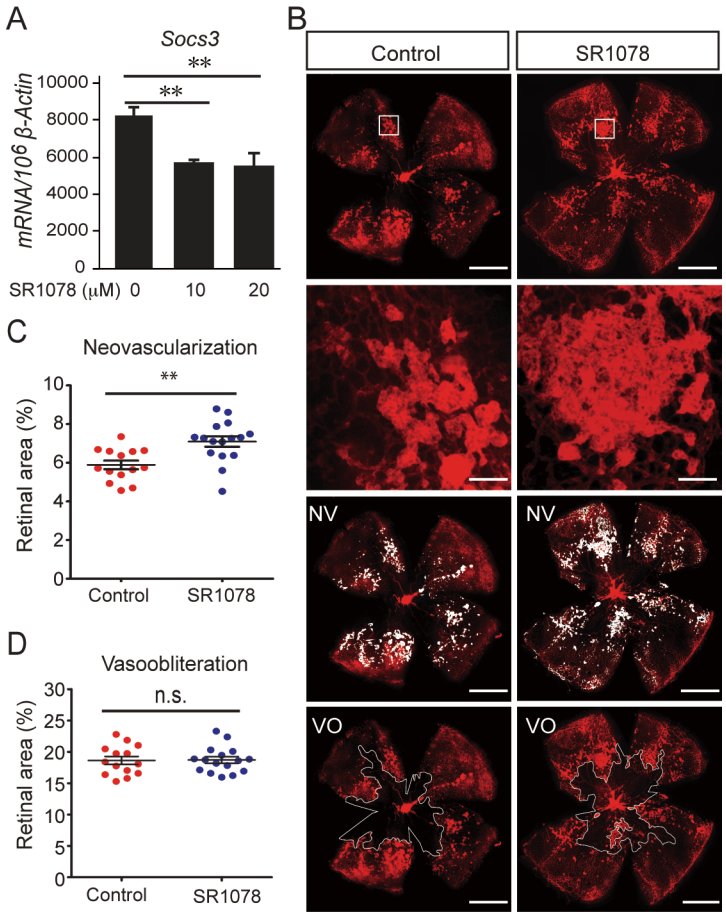

Figure S7. RORα agonist enhanced pathologic neovascularization in OIR. (**A**) RORα agonist SR1078 significantly suppressed *Socs3* expression in RAW 264.7 cells. RAW 264.7 cells were treated with 0, 10 and 20 μM of SR1078 overnight and then the cells were collected for qPCR analysis. (**B**) Representative retinal whole-mounts from P17 WT OIR mice treated with SR1078 or vehicle control were stained with isolectin IB_4 (red). Two selected retinal areas (white box) were enlarged to show pathologic neovessels. (**C**) Area of NV was highlighted (white) and quantification of pathologic NV showed significantly increased levels in SR1078 treated retinas compared with vehicle controls. (**D**) Area of VO was highlighted (white). Quantification of VO area showed comparable levels of vasoobliteration between SR1078 and vehicle control treated retinas. n=14-16/group. Scale bar: 1000 μm. **: $p<0.01$; n.s.: no significance.

Figure S8

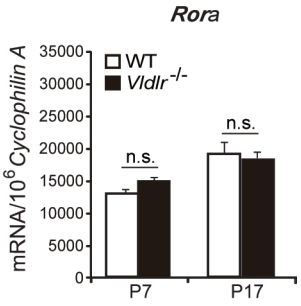

Figure S8. *Rora* expression in *Vldlr*$^{-/-}$ retinas. *Rora* mRNA expression was measured in retinas isolated from *Vldlr*$^{-/-}$ mice and compared with WT retinas with qPCR quantification (n = 3 per group). There was no significant difference between *Vldlr*$^{-/-}$ and WT at both P7 and P17. n.s., no significance.

Figure S9

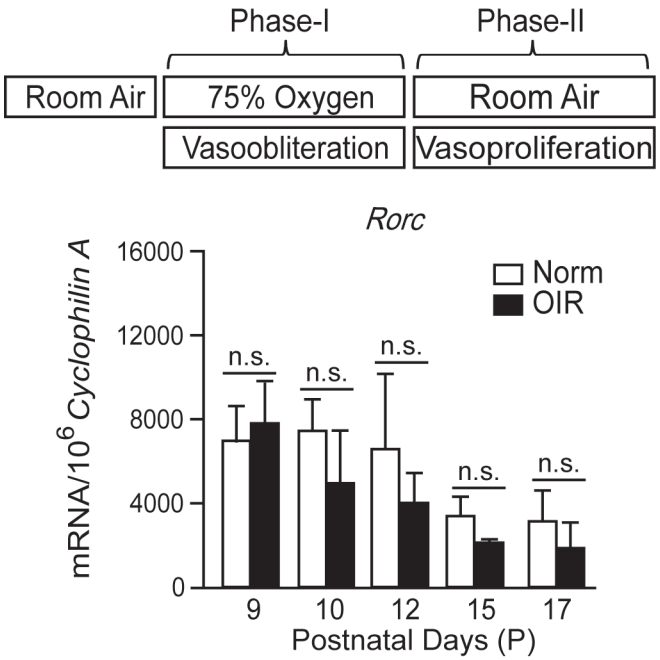

Figure S9. *Rorc* expression in OIR retinas. *Rorc* mRNA expression was measured in retinas isolated from OIR compared with age-matched normoxic control retinas with qPCR quantification (n = 6 per group), showing no significant difference between OIR and normal retinas throughout OIR. n.s., no significance.